Bidirectionally tunable all-optical switch based on multiple nano-structured resonators using backward quasi-phase-matching

Jun Xie (谢 俊), Yuping Chen (陈玉萍)*, Wenjie Lu (陆闻杰), and Xianfeng Chen (陈险峰)**

Department of Physics, State Key Laboratory on Fiber-Optic Local Area Network and Advanced Optical CommunicationSystems, Shanghai Jiaotong University, Shanghai 200240, China

**Corresponding author: ypchen@sjtu.edu.cn; **corresponding author: xfchen@sjtu.edu.cn*

Received September 20, 2010; accepted November 15, 2010; posted online March 15, 2011

Based on the second-order nonlinearity, we present a bidirectional tunable all-optical switch at C-band by introducing backward quasi-phase-matching technique in Mg-doped periodically poled lithium niobate (MgO:PPLN) waveguide with a nano-structure called multiple resonators. Two injecting forward lights and one backward propagating light interact with difference frequency generations. The transmission of forward signal and backward idler light can be modulated simultaneously with the variation of control light power based on the basic "phase shift" structure of a single resonator. In this scheme, all the results come from our simulation. The speed of this bidirectional optical switch can reach to femtosecond if a femtosecond laser is used as the control light.

OCIS codes: 190.4390, 130.3120, 130.3130, 230.1150.
doi: 10.3788/COL201109.041902

Optical switch in lightwave communication has been proposed for a long time. It aims to achieve controllable optical signals using interruption in optical paths during transmission to set optical devices on "ON" or "OFF" states. Typically, optical switch has one or several transmission windows. The function of optical switch can be implemented in several ways, such as all-optical switching in a warm laser pumped rubidium vapor or in the silicon with a micrometer-sized planar ring resonator, or ultrafast low-power photonic-crystal all-optical switching with high switching efficiency[1−3]. However, most of them can perform the optical switching function in a single direction rather than in two directions or in only a single channel rather than multiple channels, allowing them to be switchable simultaneously. In this letter, based on the second-order nonlinearity in nano-structured resonators of optical crystal, we propose a type of optical switching based on magnesium doped periodically poled lithium niobate (MgO:PPLN)[4−6], which can perform double-way modulation in a single device and carry out a simultaneous tunable bidirectional switching. Note that an all-optical wavelength conversion can also be achieved accompanied with an all-optical switching in our presented scheme, enhancing the multifunctional photonic integration in one optical device.

In this letter, we focus on the idea of back-propagation frequency conversion in quasi-phase-matching (QPM), which is used to study the slowing down of the group velocity of light beams based on the second-order nonlinearity[7]. This technique can make a large difference transmission of signal at different wavelengths. Thus, by designing the waveguide configuration, the all-optical switching of both signal and idler lights can be realized, continuously modulating the transmission of multiple wavelengths by the control light. Thus, the variety of control light can determine the adjustability of the device. The switching state for forward signal light can be transformed at a tunable signal wavelength range due to the different parameter designs in the waveguide. At the same time, the switching state can affect the backward idler, i.e., the idler state of transmission is opposite to the signal.

Figure 1 shows the schematic of the tunable optical switch, which consists of MgO:PPLN waveguide as the main body. The signal light of 1550 nm is located in the C-band of optical communication, and the control light is set to 1600 nm, which is used as a key button that can change the state of the switch to "ON" or "OFF". In Fig. 1, the signal and control lights are injected into the waveguide from the left side, and the incidence of the idler light is from the right side. The wavelength of the idler light is set to 730 nm for the backward QPM (BQPM) condition. Moreover, the other lights propagating in the waveguide should satisfy the QPM of the difference frequency generation (DFG), i.e., $\omega_{\rm i} = \omega_{\rm s} + \omega_{\rm c}$, where $\omega_{\rm i}$ is the frequency of the idler light, $\omega_{\rm s}$ is the frequency of the signal light, and $\omega_{\rm c}$ is the frequency of the control light. Moreover, the phase shift between the periodic positive and negative domains needs to be considered as well (Fig. 2). The basic structure called single resonator (SR) involves a phase shift in the sign of $\chi^{(2)}$, whose length is $2L$ and the magnitude is microscale. With two neighboring SR structures, light energy can be transmitted and reflected due to the frequency conversion and interactional energy exchange. The large number of SRs makes the linear array modulate the propagating beams in a waveguide[7−9]. Figure 2 shows the schematic of the 3.64-cm-long multiple resonator (MR) waveguide, with the waveguide length l=$2NL$, where N is the SR population and $2L$ is the unit length of SR. In this kind of waveguide, we consider two segments of equal length L in a SR but with the reversed signs of $\chi^{(2)}$ as the "phase shift" of QPM. It is equivalent to a Fabry-Perot cavity with nonlinear mirror, which introduces the phase

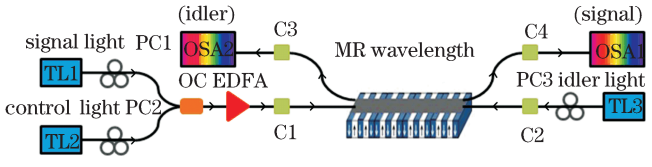

Fig. 1. Schematic diagram of a tunable all-optical switch with MR in a MgO:PPLN waveguide. TL: tunable laser; PC: polarization controller; OC: optical coupler; EDFA: erbium-doped fiber amplifier; C: collimator; OSA: optical spectral analyzer.

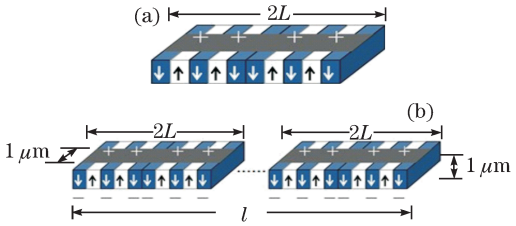

Fig. 2. Schematic diagram of nano-structured resonators. (a) SR consisting of the BQPM waveguide, where the sign of $\chi^{(2)}$ reverses periodically with one phase shift in the middle; (b) MR consisting of a large number of SR. In our simulation, N = 30, L = 606.7 μm, and the effective transverse area of MR waveguide is $S_{\rm w}$ =1 μm^2.

shift of the nonlinear coefficient d_{31}[7]. In the cavity, the forward-propagating photons with a frequency ω_0 will be reflected as backward-propagating photons with the new resonant frequency $\omega_0' = \omega_0 + \omega_{\rm c}$ satisfying the DFG condition. These behaviors of the forward light and backward light are both similar to those when they propagate in the waveguide, satisfying the Bragg condition. The energy flow of the forward light is continuously transferred to the backward light with the variation in control light power based on the "phase shift" structure in SR. The function of a large number of SRs is considered a coupled BQPM MR; thus, this kind of waveguide structure can engender two high reflectivity bands for the incident forward light and two high transmission bands for the incident backward light in the spectrum, respectively[10]. Hence, this characteristic of MR waveguide can be utilized to implement tunable optical switching.

Assuming all lights to be TM polarization, a set of coupled equations for counterpropagating waves in the DFG process is derived as follows:

$$\begin{aligned} \frac{{\rm d}A_{\rm s}}{{\rm d}z} &= \kappa A_{\rm i} {\rm e}^{{\rm j}2\Delta\beta z}, \\ \frac{{\rm d}A_{\rm i}}{{\rm d}z} &= \kappa A_{\rm s} {\rm e}^{-{\rm j}2\Delta\beta z}, \end{aligned} \tag{1}$$

where $A_{\rm s}$, $A_{\rm i}$ represent the electric fields of the signal and idler, respectively. The total phase mismatching is

$$\Delta\beta = \beta_{\rm s} + \beta_{\rm i} + \beta_{\rm c} - 2\pi/\Lambda, \tag{2}$$

where $\beta_{\rm s}$, $\beta_{\rm i}$, and $\beta_{\rm c}$ are the propagation constants associated with $\omega_{\rm s}$, $\omega_{\rm i}$, and $\omega_{\rm c}$, respectively, which are the angular frequencies of signal, idler, and control lights; Λ is the poling period of BQPM.

In Eq. (1), the coupling coefficient can be expressed as

$$\kappa = \frac{4}{\pi}\frac{d_{31}}{c}\sqrt{\frac{\omega_{\rm s}\omega_{\rm i}}{n_{\rm s}n_{\rm i}n_{\rm c}}\eta_0\frac{P_{\rm c}}{S_{\rm w}}}, \tag{3}$$

where $P_{\rm c}$ is the control power, η_0 is the vacuum impedance, $S_{\rm w}$ is the effective transverse area of the waveguide, and $n_{\rm s}$, $n_{\rm i}$, $n_{\rm c}$ are the refractive indices of the signal, idler, and control lights, respectively. In our scheme, we choose 1550 and 730 nm as the wavelengths of the signal light and the idler light, respectively. Thus, N = 30 and L = 606.7 μm. Λ is equal to 182 nm to satisfy Eq. (2), where the grating period of 182 nm is too small to be fabricated in our laboratory currently. However, the precision nanoscale domain engineering of lithium niobate through ultraviolet laser-induced inhibition of poling has been realized[11], which can make the proposal of the nano-structured resonators in this letter feasible.

To characterize the MR waveguide structure, we first calculate the reflection and transmission coefficients of this device as[7,12–14]

$$\begin{aligned} r &= \frac{A_{\rm i}(0)}{A_{\rm s}(0)} = -\frac{\kappa}{s}\frac{\tanh sl}{1 + {\rm j}\frac{\Delta\beta}{s}\tanh sl}, \\ t &= \frac{A_{\rm s}(L)}{A_{\rm s}(0)} = \frac{\cosh^{-1} sl}{1 + {\rm j}\frac{\Delta\beta}{s}\tanh sl}, \end{aligned} \tag{4}$$

where $s = \sqrt{\kappa^2 - (\Delta\beta)^2}$.

To illustrate how to realize a tunable bidirectional all-optical switch in this structure, we investigate the power of the signal and idler dependent on the power of control light by tuning the signal from 1548 to 1552 nm, where the control light and idler are fixed at 1600 and 730 nm, respectively. To solve the mode matching problem in the waveguide, we can generate idler light at 730 nm through broadband QPM second harmonic generation[5] by inputting 1460-nm wavelength[15]. There are two types of PPLN waveguides that can be utilized in optical communications: proton-exchanged PPLN waveguide, which can be doped by Mg[15], and titanium-diffused PPLN waveguide[16]. In our scheme, the MR waveguide sample for the optical switch with the length of 3.64 cm can be fabricated by the first method, where the crystal sample $LiNbO_3$ is dealt with by the electrical poling method and is thereafter annealed by the proton-exchanged process. Here, we assume that the waveguide sample is a 3.64-cm-long lithium niobate crystal, with the effective area of the waveguide as $S_{\rm w}$ = 1 μm^2, $n_{\rm i}$ = 2.1681, $n_{\rm c}$ = 2.1285. Figure 3 (colorful online) shows the normalized output profiles of signal light and idler light in the MR waveguide. The cold-color region represents low power, whereas the warm-color region denotes high power. At the edge of the blue and red regions, the change in all-optical switch states "ON" or "OFF" can be carried out by manipulating the power of the control light. In Fig. 3(a), by increasing the control power, the normalized output power of the signal is maintained at a near zero value when the wavelength is 1550.7 or 1549.2 nm. The blue region represents the near zero value of the control power and is stretched in the signal profile. At the signals of λ_1 = 1549 nm and λ_2 = 1551 nm, the normalized output power of the idler light is almost 1 (Fig. 3(b)) and shows a performance opposite to that in Fig. 3(a). Note that the located areas of the output power of signal (Fig.

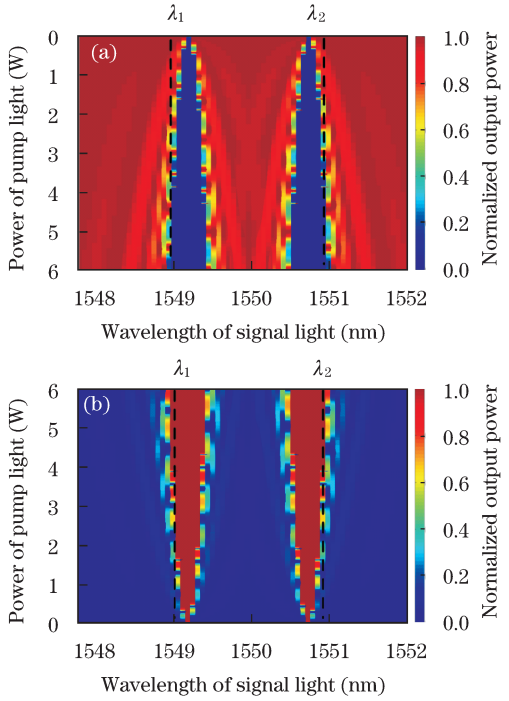

Fig. 3. Normalized output power of (a) signal light and (b) idler light with variable powers of pump light in different signal wavelengths, where $\lambda_1 = 1549$ nm and $\lambda_2 = 1551$ nm.

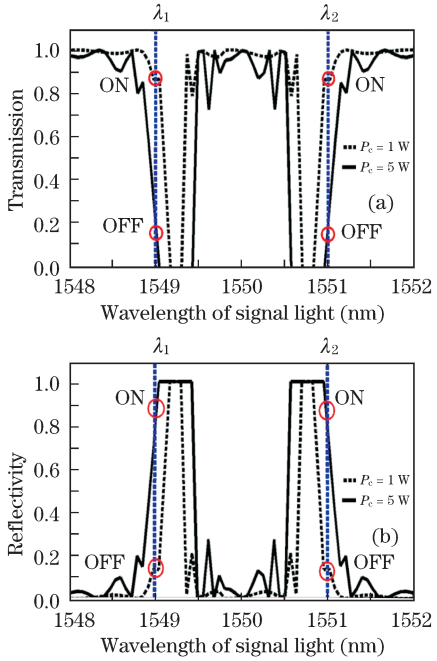

Fig. 4. Characteristic of the MR waveguide under two different control powers $P_c = 1$ and 5 W. (a) Transmission of signal light; (b) reflectivity of idler light.

3(a)) and idler (Fig. 3(b)) have the normalized values of "1" to "0" as shown on the bar in Fig. 3. They are dependent on the wavelength of the signal and the input power of the control light, which make up the conditions of all-optical switching.

In our proposal, the wavelength of the signal light at the edge is about 1549 or 1551 nm. If the power of the control light is increased from 1 to 5 W, a great contrast in the transmission of signal can be produced (from "ON" state to "OFF", as shown in Fig. 4(a)); the same occurs for the reflectivity of the idler (from "OFF" state to "ON", as shown in Fig. 4(b)). Using the characteristics of transmission between the signal and idler, a "bidirectional optical switch" can be performed in the MR structure simultaneously.

In Fig. 4(a), selecting the signal wavelength of 1549 and 1551 nm, respectively, when $P_c = 1$ W, the transmission of signal is 0.87. Increasing the control power to 5 W, the transmission of signal is decreased to 0.13, which means that the signal changes from the "ON" state to the "OFF" state. The extinction ratio is defined as $R_e = 10\lg(P_{ON}/P_{OFF})$, where P_{ON} and P_{OFF} are the "ON" and "OFF" normalized optical powers; in Fig. 4(a), it emerges at 8 dB. The corresponding "ON" state for P_c =1 W is at the wavelengths of λ_1 and λ_2, whereas the "OFF" state for $P_c = 5$ W lies in the same wavelength as the previously "ON" state.

In Fig. 4(b), assuming no loss in the optical crystal, the transmission of idler varies from 0.13 to 0.87 at the signal wavelength of 1549 or 1551 nm. The idler goes from the "OFF" state for P_c =1 W to the "ON" state for P_c = 5 W. By comparing the simulated results in Figs. 3 and 4, the responses of the two beams (i.e., signal and idler) have the similar and opposite characteristics. The state of the idler switches from "OFF" to "ON" once the control power is changed to 5 W. Evidently, the same situation occurs in the "OFF" state of the signal. Thus, the variety of control light can determine the adjustability of the device. The switching to forward signal light can be transformed from one single wavelength to another depending on the different parameter designs of the waveguide. At the same time, it can affect the behavior of the switching of backward idler, i.e., the idler state of transmission is opposite to the signal.

Considering the fabrication errors in the grating spacing dependence on sensitivity, these errors in the nonlinear frequency conversion efficiency of signal or idler are proportional to the length of the device[17], which is 3.64 cm in our design, whereas the fabrication errors' magnitude is less than 1 μm. Thus, the sensitivity dependence on grating errors has 10^{-4} orders of magnitude, which has no influence on the switching performance. We also study the wavelength sensitivity of MR optical switching. If the transmission of signal or idler is less than 50%, the switch can be considered invalid. Thus, in Fig. 4, the maximum wavelength drift is less than 0.1 nm to make the switch available when using the 3.64-cm-long waveguide sample, which requires high long-term stability for the input lasers. The bandwidth of our switch is related to κ in Eq. (3). By increasing the value of κ, we can obtain a wider bandwidth using a larger control power or a smaller effective area of the waveguide. However, with the increase in control power, the maximum wavelength drift of the signal light allowed for the device can increase up to 0.3 nm for $P_{ON} = 1$ W and $P_{OFF} = 10$ W.

In conclusion, we present a new method to achieve a bidirectional all-optical switch with the BQPM technique in a MgO:PPLN waveguide. In our simulation, three separated light beams go through the waveguide with different phenomena, which can carry out bi-passing optical switching at the C-band. The second-order QPM

nonlinear conditions and the power of control light provide the key contributions to the entire scheme. This bidirectional all-optical switching has potential applications in optical integrated circuits in the future.

This work was supported by the National "863" Program of China (No. 2007AA01Z273), the National Natural Science Fundation of China (No. 10874120), and the Scientific Research Foundation for the Returned Overseas Chinese Scholars, Ministry of Education of China.

References

1. A. M. C. Dawes, L. Illing, S. M. Clark, and D. J. Gauthier, Science **308,** 672 (2005).
2. V. R. Almeida, C. A. Barrios, R. R. Panepucci, M. Lipson, M. A. Foster, D. G. Ouzounov, and A. L. Gaeta, Opt. Lett. **29,** 2867 (2004).
3. X. Hu, P. Jiang, C. Ding, H. Yang, and Q. Gong, Nature Photon. **2,** 185 (2008).
4. Y. Chen, R. Wu, X. Zeng, Y. Xia, and X. Chen, Opt. Laser Technol. **38,** 19 (2006).
5. J. Zhang, Y. Chen, F. Lu, and X. Chen, Opt. Express **16,** 6957 (2008).
6. K. Liu, J. Shi, and X. Chen, Opt. Lett. **34,** 1051 (2009).
7. J. B. Khurgin, Phys. Rev. A **72,** 023810 (2005).
8. X. Gu, M. Makarov, Y. J. Ding, J. B. Khurgin, and W. P. Risk, Opt. Lett. **24,** 127 (1999).
9. C. Canalias, V. Pasiskevicius, M. Fokine, and F. Laurell, Appl. Phys. Lett. **86,** 181105 (2005).
10. M. F. Yanik and S. Fan, Phys. Rev. Lett. **92,** 083901 (2004).
11. C. L. Sones, A. C. Muir, Y. J. Ying, S. Mailis, R. W. Eason, T. Jungk, Á. Hoffmann, and E. Soergel, Appl. Phys. Lett. **92,** 072905 (2008).
12. A. Yariv, *Optical Electronics in Modern Communications* (Oxford University Press, New York, 1997), pp. 509-510.
13. J. B. Khurgin, J. Opt. Soc. Am. B **22,** 1062 (2005).
14. A. Melloni, F. Morichetti, and M. Martinelli, Opt. Quantum Electron. **35,** 365 (2003).
15. M. H. Chou, I. Brener, M. M. Fejer, E. E. Chaban, and S. B. Christman, IEEE Photon. Technol. Lett. **11,** 653 (1999).
16. H. Kanbara, H. Itoh, M. Asobe, K. Noguchi, H. Miyazawa, T. Yanagawa, and I. Yokkohama, IEEE Photon. Technol. Lett. **11,** 328 (1999).
17. Y. Kong, X. Chen, and Y. Xia, Appl. Phys. B **91,** 479 (2008).